SLAC-PUB-659
November 1969
(ACC)

LINAC BEAM INTERACTIONS AND INSTABILITIES*

G. A. Loew, R. H. Helm, H. A. Hogg, R. F. Koontz, and R. H. Miller

Stanford Linear Accelerator Center
Stanford University, Stanford, California 94305

I. Introduction

The electron beam which is accelerated in the SLAC two-mile accelerator exhibits both transverse and longitudinal interactions with the disk-loaded waveguide. The transverse interactions include such effects as rf steering caused by field asymmetries which exist in the couplers, and beam breakup. The latter is a growing instability which occurs above a given current threshold and deflects the beam into the walls of the machine. The longitudinal interactions include bunching, acceleration and the general phenomenon of beam loading which causes spectrum broadening. Both beam breakup and beam loading are basically detrimental to the use of the beam and must be controlled or compensated for. Beam breakup, especially, is affected by the manner in which the beam is formed in the injector, and in particular by its time structure, i.e., whether the train of bunches is continuous or chopped.

The purpose of this paper is to review some of the recent work done on the beam breakup and beam loading phenomena at SLAC. The review includes a description of the present beam chopping system and its associated instrumentation. The problems of beam breakup in a two-mile superconducting linac are also briefly considered. Finally, the reader will find the description of an experiment, uncompleted so far, which uses the beam loading phenomenon and highly sensitive phase detection equipment to measure the velocity difference between two relativistic beams of different energies.

II. Beam Breakup

As illustrated in Fig. 1 and discussed by many authors (see for example Refs. 1-10), the beam breakup effect in electron linacs can manifest itself in two different forms: regenerative and cumulative. Both are caused by interaction of the beam with the HEM_{11} mode in the disk-loaded waveguide. Both start from noise which consists of or results in a small transverse modulation of the electron bunches at the breakup frequency. However, the growth mechanisms are different. Regenerative breakup, illustrated in Fig. 1a, occurs in one section and requires some form of feedback for build-up. Consider a noise generated HEM_{11} wave traveling with a phase velocity in the same direction as the electrons but slightly slower than them so that they slip by 180° in their travel along the accelerator section. In the first half, the phase of the wave is such that the force on the electrons due to the HEM_{11} fields is strongly deflecting. As they get deflected, they also slip ahead in phase and in the second half of the section, they find themselves in a longitudinally decelerating field to which they give up energy. If the mode is of the backward-wave type or if there are reflections, this energy travels back upstream where it reinforces the original deflecting field. Above a given starting current and pulse length, the process becomes regenerative; both the field and the deflection grow exponentially, and the beam is lost.

In contrast, the cumulative multisection type of breakup is illustrated in Fig. 1b. Here, because of the same initial transverse modulation on the beam, small HEM_{11} resonances build up in individual accelerator sections. As a result, later electron bunches which see these fields receive an additional amount of transverse momentum which over a given distance translates itself into displacement modulation. This modulation further excites the resonant fields in the downstream cavities and these, in turn, deflect the bunches even more until finally they scrape the accelerator walls. Within each beam pulse, the effect is coherent and cumulative as a function of length and time.

The phenomenon of cumulative beam breakup was first experienced in the 2 GeV electron linac at Kharkov.[1] Subsequently, the same phenomenon appeared at the SLAC two-mile accelerator, shortly after the machine was turned on in 1966. It has been the subject of intensive study ever since.[2,5-10] While the single-section regenerative effect requires starting beam currents in the ampere range, the cumulative effect at first limited beam operation at SLAC to 20 mA at 1.6 μsec pulse length. As a result of several improvement programs described below, the threshold has now been raised to 65 mA under optimized machine tuning conditions. By the time the present program is completed, this threshold should reach 80 to 90 mA.

Several essentially equivalent theoretical treatments of cumulative beam breakup have been given (for a review of these treatments, see Ref. 9). The simplest transient solution, representing the response to an initial delta-function of transverse disturbance in an accelerator without focusing, may be expressed as

$$x(z,t) \approx x_0 e^{F}$$

$$\approx x_0 \exp\left\{\left[CIt\left(\int_0^z \gamma^{-1/2}dz\right)^2\right]^{1/3} - \frac{1}{2}\omega_1 t/Q\right\}$$

where x is the transverse displacement amplitude, x_0, the initial value, is a slow function related to the initial impulse, t is time, I is the current, ω_1 and Q are the frequency and quality factors of the HEM_{11} resonance, C is a geometric factor proportional to the shunt impedance of the HEM_{11} mode divided by Q, and γ is the normalized energy. Experience at SLAC indicates that breakup occurs when the e-folding factor F is on the order of 15.

As a result of experimental, analytic and computer studies, it was predicted that the breakup threshold at SLAC could be improved in several ways. The first improvement program involved strengthening the focusing

*Work supported by U.S. Atomic Energy Commission.

(7th Int. Conf. on High Energy Accelerators, Yerevan, Armenia, USSR, Aug. 27-Sept. 2, 1969)

system. Originally, this system employed quadrupole triplets at sector intervals (one sector is one-thirtieth of the machine, or about 100 m). It was capable of maintaining the optimum four-sector betatron wavelength (λ_β) for the first seven sectors but was limited to constant quadrupole strength thereafter. The quadrupoles were then rearranged so that there were eight equally spaced alternating gradient singlets per sector for the first six sectors, and quadrupole doublets at sector spacing in the remainder of the machine. At full machine energy, this system operates at λ_β = 150 m in the first six sectors, λ_β = 400 m from sector 6 to about sector 24, and constant quadrupole strength thereafter. When this rearrangement was completed in 1967, the breakup threshold was improved from the original 20 mA to about 40 mA (see Table 1 and Fig. 2).

The next improvement program at SLAC, which is still in progress, is based on shifting the HEM_{11} resonant frequency (4139.6 MHz) by detuning selected portions of the machine. This detuning operation is feasible because in the SLAC tapered constant-gradient structure, the HEM_{11} resonance occurs only in the first few cavities of each 86-cavity section. Hence, by physically "dimpling" (i.e., deforming or squeezing) cavities 3, 4 and 5 of each section, it is possible to shift the transverse resonance by several MHz (typically 2 or 4 MHz) with an almost negligible effect on the accelerating properties of the section (correspondingly four or eight degrees per cavity at 2856 MHz) or the VSWR (typically < 1.1).

Favorable choices of which sectors to detune by 4, 2 or 0 MHz were determined by means of computer calculations. Some of these detuning schedules are illustrated in Fig. 3. The nomenclature for curves A, B and C is as follows:

Curve A: + 4 MHz, Sectors 1, 2, 7, 8, 13, 14, 19, 20, ...
+ 2 MHz, Sectors 3, 4, 9, 10, 15, 16, ...
0 MHz, Sectors 5, 6, 11, 12, 17, 18, ...
(i.e., 442200, 442200, ...)

Curve B: + 4 MHz, Sectors 1, 2, 9, 12, 15, 18, ...
+ 2 MHz, Sectors 3, 4, 5, 10, 13, 16, ...
0 MHz, Sectors 6, 7, 8, 11, 14, 17, ...
(i.e., 4422200, 042, 042, ...)

Curve C: + 4 MHz, Sectors 1, 2, 12, 15, 18, ...
+ 2 MHz, Sectors 3, 4, 5, 13, 16, 19, ...
0 MHz, Sectors 6, 7, 8, 9, 10, 11, 14, 17, 20, ...
(i.e., 4422200000, 042, 042, ...)

Schedule C has been adopted and is presently being implemented (see Table 1 and Fig. 2 for the progressive improvements to date). The tool used to produce the "dimpling" is shown in Fig. 4. It consists of four small plungers at 90° whose degree of insertion is controlled by a pre-set screw adjustment. The rate of insertion is controlled by a hydraulic system (see Fig. 5). At first the operation was monitored with a microwave phase bridge but when it was verified that the frequency shift could be controlled to better than 10% through proper use of the tool, "dimpling" was done directly, without even letting the accelerator down to air. Figure 6 shows typical HEM_{11} resonances in a ten-foot section in sector 1, before and after detuning by 4 MHz. The double peaks represent the vertical (higher Q) and horizontal (lower Q) resonances caused by the coupler configuration.

A complete beam breakup plot of charge and current vs. pulse length for the entire accelerator under optimum focusing conditions is shown in Fig. 7. When compared with earlier similar curves taken at SLAC, it is seen that the improvement obtained through selective detuning is only apparent for pulse lengths greater than 0.6 μsec. This is understandable since, for shorter pulses, the resonant buildup has insufficient time to take place.

Any further improvement will have to result from additional focusing. A program is presently underway to add pulsed quadrupoles in some of the drift sections of the accelerator. The first pulsed doublet (see Fig. 8) has been installed in sector 28. Although the main purpose of these pulsed lenses is to produce special focusing conditions on a pulse-to-pulse basis, their use in the last six sectors of the machine should ultimately raise the breakup threshold to 86 mA (see Table 1).

Attempts to reduce the initial noise have been made (rf filters in the klystron outputs, small gun cathode) but so far have produced no substantial improvement. In fact, when chopped beams are used as described in the next section of this paper, the beam breakup threshold is decreased as the rejection ratio (or charge per bunch) is increased (see Fig. 9).

In connection with the feasibility study of the two-mile superconducting linac,[11] some consideration has been given to the beam breakup problems in such a machine. Under the typical high duty factor and long pulse operation, beam breakup would take place under steady-state conditions. Analysis of steady-state breakup shows that the behavior of the e-folding factor is $F \propto (QIz/\gamma')^{1/2}$ where focusing has been neglected. Numerical evaluation shows that a value of $Q \lesssim 10^5$ would be required to attain the objectives assumed in the study. Since superconducting Q's are expected to be on the order of 10^9 to 10^{10}, it would seem necessary to lower the Q of the breakup mode by selectively loading the structure. However, the above result assumes that all parts of the machine are identical; actually it is expected that the resonant frequency of the breakup mode will vary in different sections of the machine by a relative amount comparable to fabrication tolerances (i.e., on the order of one part in 10^4). This lack of coherence should be very similar to lowering the effective Q. Further analysis and computer studies of these problems will be required.

The superconducting machine will also be expected to operate in a short pulse, high peak current mode. The beam breakup limit will then occur under highly transient rather than steady-state conditions. In this case, the breakup threshold is insensitive to the Q of the interaction. The most effective means of suppression then seem to be (a) use of several structure modifications so that the interaction takes place at frequencies separated by at least several MHz, in different parts of the machine, and (b) use of a fairly strong focusing system.

III. The Chopped Beam System, Principle and Performance

A variety of chopped beams has been in demand for various experiments at SLAC in the past years. Chopping and monitoring equipment has been growing steadily more complex. Figure 10 is a block diagram of the system as it now exists, except for the fast pulser which will be installed shortly. Table 2 lists the capability of this equipment.

The primary chopping equipment consists of two 50 kW rf amplifiers, one tuned to 39.667 MHz (the 72 subharmonic of the accelerator frequency), the other variable in tuning from 5 to 20 MHz. The 39.667 MHz amplifier drives a set of resonant chopper plates just downstream of the gun (50-80 kV) and prebuncher. These plates can chop the beam into single or multiple bunch pulses with a basic spacing of 12.5 nanoseconds. The length of this pulse train is determined by the slow pulser which modulates the gun cathode. The degree of chopping is determined by the power applied to the plates.

The 5 to 20 MHz amplifier drives a set of nonresonant traveling-wave deflection plates located 15 feet downstream of the gun, at a beam energy of 40 MeV. These plates can be operated at frequencies which are subharmonics of 39.667 MHz, to produce pulse spacings of 25, 50 or 100 nanoseconds. They can also be operated at any frequency between 5 and 20 MHz, unsynchronized to the machine frequency, to produce multibunch pulse trains of variable spacing.

Occasionally accelerator operation calls for two interlaced chopped beams with different pulse train spacings. When the spacings have a 2 to 1 ratio, a set of pulsed steering magnets at the second deflector can be used. When off, it allows bunches to be transmitted at the rf field zero crossings (two bunches per cycle) and when on, it transmits them at the peaks of the rf field (1 bunch per cycle).

Many of the functions of the downstream deflector plates and the pulsed magnet will be taken over by a fast gun grid pulser soon to be installed. This pulser can generate trains of 2-nanosecond pulses with spacings of any multiple of 12.5 nanoseconds. Up to three different spacings can be selected on a pulse-to-pulse basis. The pulser can be used alone to produce trains of 2 nanosecond pulses or in conjunction with the 39.667 MHz first deflector to produce single bunch pulse trains.

The chopped beams described here are monitored by means of two ferrite-core, single-turn toroids (one in the injector, the other in sector 27). Both are connected directly to viewing scopes by means of air dielectric coaxial cable. They can resolve pulses separated by more than 2 nanoseconds. Below this limit, in order to differentiate between single and double (adjacent) bunch trains, a special monitor and sampling scope system has been installed in sector 10 (see Fig. 11). A one-inch ceramic tube has been inserted along the beam pipe. This discontinuity serves to launch an electromagnetic wave proportional to the beam pulse intensity on a slab line and high quality coaxial cable. This cable terminates in a sampling scope which can be monitored outside the radiation area. The ferrite cores on axis act as high frequency chokes. The monitor has a rise time of about 200 picoseconds and can differentiate between adjacent bunches in the beam pulse. Its response is flat down to about 100 kHz but at this stage of development, the device still exhibits some undesirable reflections.

Also shown in Fig. 10 is the main drive line supplying 476 MHz cw power to the entire klystron gallery. This line can also be used to transmit 1-50 MHz synchronization signals from the chopper system to any of the experimental areas.

While this entire system has given excellent performance, two problems have so far remained unsolved. The first is the reduction in beam breakup threshold with chopping strength, mentioned earlier and illustrated in Fig. 9. This effect is caused by the increased initial shock excitation of the more highly charged bunches. The second is the increased spectrum width, shown in Fig. 12, for a chopped beam as compared to a regular beam of the same intensity. This effect, which can be somewhat disturbing to an experimenter, has not yet been clearly understood. Neither has it been understood why the net energy for the chopped beam seems to be lower by about 0.3%. After several other explanations had been temporarily discarded (greater bunch width, increased conventional beam loading in the injector), it was thought that the time structure of the pulse train could cause beam loading sidebands at discrete frequencies such as 2856 ± 20 MHz, ± 40 MHz, ± 60 MHz, etc. The experimentally measured spectrum shown in Fig. 13 actually confirmed the existence of these sidebands but calculations made so far seem to show that the levels are insufficient to explain the observed spectrum broadening. Further work will have to be done on this problem.

IV. Energy Transient Compensation

The phenomenon of beam loading as it manifests itself in the SLAC accelerator is well known.[14] Increasing the operating beam current not only depresses the electron energy; it also broadens the energy spectrum because the net accelerating fields exhibit ripples and decrease during the transient period at the beginning of the beam pulse. The high-energy tail on the spectrum becomes increasingly long and undesirable as the beam current is raised.

First-order compensation for the transient beam-loading energy spread is obtained by delaying the klystron turn-on time in one or more sectors of the accelerator. The rising fields in the accelerator pipes supplied by these klystrons then approximately balance the falling beam energy due to transient loading in the rest of the accelerator. The balance is less than perfect, however, because the leading edges of the beam-loading waveform and the delayed accelerating voltage waveform do not follow the same law. Thus, when the beam is analyzed and transmitted through narrow slits, a depression or "gulch" is often observed near the middle of the current pulse, as shown in Fig. 14.

It is possible to fill the "gulch" by adding a short accelerating pulse of the correct amplitude, shape and timing. This compensating pulse could be generated, for instance, by energizing short accelerator sections (each having a filling time less than half the gulch width).

However, it has been possible to produce the desired pulse length using standard SLAC 10-foot accelerator sections. The method is illustrated in Fig. 15. The incoming beam pulse is assumed to be mono-energetic, with the exception of a triangular "gulch" beginning at t_2 and ending at t_4. The first compensator section receives a klystron rf pulse of length $(t_3 - t_2)$. As this pulse enters the section, it compensates for the first half of the triangular gulch, as shown. However, because of the long section filling time (0.83 μsec), the energy vs. time waveform of the emergent beam, V_1, has an upward step at the end of the pulse. This "overshoot" is corrected in the following accelerator section which is energized by an rf pulse beginning at t_3 and ending at t_4. The rf wave is appropriately phased to decelerate the beam, cancelling the energy overshoot at the end of the beam pulse.

The method described above has been tried at SLAC and works quite well; Fig. 14 shows the degree of compensation achieved with a 17 GeV beam analyzed through 0.2% slits. The rf drive to two adjacent klystrons is gated by means of fast, high-power PIN diode switches. Each switch is a strip-line assembly containing two diodes which shunt the rf through quarter-wave and half-wave stubs. The switch is closed by triggering the "quarter-wave" diode into conduction, and opened by triggering the "half-wave" diode into conduction. Thus, the delay and width of the gated rf pulse can be controlled by separately varying the delays on the two triggers. Both diodes revert to their non-conducting states during the inter-pulse period. The optimization of rf phase, pulse width and delay for the two klystrons is done experimentally, while watching a display of the analyzed beam.

The method discussed here has the disadvantage that the two klystrons are run at reduced drive power. Thus, their beam powers are largely wasted in their collectors. The same compensation could be achieved more efficiently by employing fast PIN diode SPDT switches to pulse-modulate the phase of the rf drive at the appropriate time during the beam pulse. A third possibility is to use varactor phase-shifters. The state of the art on these devices is just reaching the point where large transmission phase shifts can be obtained with minimal changes in insertion loss.

V. Measurement of Velocity Difference Between Two Relativistic Electron Beams

Experience with operation of the two-mile accelerator combined with a proposal to measure the velocity difference between two photon beams at SLAC[15] recently prompted the idea for the experiment illustrated in Fig. 16. The principle is as follows. Let a "high energy" (6 GeV) and a "low energy" (0.5 GeV) beam be accelerated in the first third of the machine. Then, let them both drift from sector 10 to sector 30. At both sectors 10 and 30, install highly sensitive phase bridges and compare the phases of the two beam-induced signals (in a short cavity or accelerator section) with the rf drive line signal. Assuming currents of the order of a mA (giving negligible beam loading) and stable overall conditions, the difference in phase between the two beams and the drive line signal (coherent with the beam) should yield the difference in velocity between the two beams. If v_1 and v_2 are the respective velocities, and t_1 and t_2 the times of flight, given a length ℓ we obtain:

$$t_1 = \ell/v_1 \qquad v_1/c = 1 - \frac{1}{2\gamma_1^2}$$

$$t_2 = \ell/v_2 \qquad v_2/c = 1 - \frac{1}{2\gamma_2^2}$$

$$t_1 - t_2 = \left(\frac{1}{2\gamma_1^2} - \frac{1}{2\gamma_2^2}\right)\frac{\ell}{c}$$

If γ_2 is large, the time difference becomes simply $\Delta t = (1/2\gamma_1^2)\,\ell/c$ where γ_1 is the normalized energy of the low energy beam. For 2 km, $\ell/c \approx 7 \times 10^6$ picoseconds and for 0.5 GeV, $\Delta t \approx 3.5$ picoseconds. At 2856 MHz, one electrical degree corresponds to about one picosecond; consequently, the phase bridges must be able to resolve on the order of 0.35° to give a 10% measurement of Δt. This they can achieve fairly easily.

While this experiment has not yet been done in its final form, initial measurements indicate that overall phase stability is quite good and that the experiment should be reasonably easy to perform. There is, of course, no a priori reason to suspect that the theory of relativity will not once more be verified. The experiment is mostly done as an amusing exercise.

Acknowledgements

The authors are indebted to the accelerator operators for their help in setting up the various beams required for these experiments, T. C. McKinney for his invaluable help in all the microwave measurements, A. Lisin, R. Sandkuhle and E. Frei for their help in the mechanical task of detuning the accelerator sections and installing magnets and Z. D. Farkas for his research on microwave diodes.

References

1. A. K. Valter, I. A. Grishayev, E. V. Eremenko, J. I. Dobroljubov, A. I. Zykov, V. V. Kondratenko, G. F. Kuznetzov, J. M. Bazajev, F. A. Goroshovatsky, V. B. Mufel, N. I. Motcheshnikov, V. V. Petrenko, V. I. Kolosov, N. A. Kovalenko, G. A. Zeitlenok, V. M. Levin, I. F. Malishev, E. G. Komar, V. V. Rumjantzev, F. F. Turkin, and V. K. Chochlov, "2 GeV traveling wave electron accelerator," Proceedings of the Fifth International Conference on High Energy Accelerators, Frascati, Italy (1965); pp. 233-238.

2. O. H. Altenmueller, E. V. Farinholt, Z. D. Farkas, W. B. Herrmannsfeldt, H. A. Hogg, R. F. Koontz, C. J. Kruse, G. A. Loew, and R. H. Miller, "Beam breakup experiments at SLAC," Proceedings of the 1966 Linear Accelerator Conference, Los Alamos, New Mexico (1966).

3. G. V. Voskresensky, V. I. Koroza, and Y. N. Serebryakov, "Toward the investigation of the radial instability of a beam in a linear electron accelerator," Uskoriteli (Accelerators), Vol. 9, Moscow Institute of Engineering Physics, Atomizdat, Moscow, U.S.S.R. (1966).

4. G. V. Voskresensky and Y. N. Serebryakov, "Dynamics of transverse instability of a beam in linear electron accelerator," Proceedings of the Sixth International Conference on High Energy Accelerators, Cambridge Electron Accelerator, Cambridge, Massachusetts, CEAL-2000 (1967); p. A-46.

5. G. A. Loew, IEEE Transactions on Nuclear Science NS-14, 529 (1967).

6. W.K.H. Panofsky and M. Bander, Rev. Sci. Instr. 39, 206 (1968).

7. R. H. Helm, G. A. Loew, and W.K.H. Panofsky, "Beam dynamics," The Stanford Two-Mile Linear Accelerator, Edited by R. B. Neal (W. A. Benjamin, Inc., New York, 1968), Chapter 7.

8. R. H. Helm, G. A. Loew, R. H. Miller, and R. B. Neal, "Recent developments at SLAC," Proceedings of the 1968 Proton Linear Accelerator Conference, Brookhaven National Laboratory, New York (1968).

9. R. H. Helm and G. A. Loew, "Beam breakup," Stanford Linear Accelerator Center, Stanford University, Stanford, California, Report No. SLAC-DOC-110 (1968). Also: R. H. Helm and G. A. Loew, "Beam breakup," Linear Accelerators, Edited by P. M. Lapostolle and A. Septier (North-Holland Publishing Company, Amsterdam, 1969); Chapter B.1.4 (to be published).

10. R. H. Helm, H. A. Hogg, R. F. Koontz, G. A. Loew, R. H. Miller and R. B. Neal, "Recent beam performance and developments at SLAC," Proceedings of 1969 National Particle Accelerator Conference, Washington, D.C., IEEE Transactions on Nuclear Science (to be published).

11. W. B. Herrmannsfeldt, G. A. Loew, and R. B. Neal, "Two-mile superconducting accelerator study," Proceedings of the 7th International Conference on High Energy Accelerators, Yerevan, Armenia, U.S.S.R. (1969) (to be published).

12. P. B. Wilson, "A simple analysis of cumulative beam break-up for the steady-state case," High Energy Physics Laboratory, Stanford University, Stanford, California, Report No. HEPL-TN-67-8 (1967).

13. R. H. Helm, "Preliminary estimate of beam blow-up for a superconducting electron linac," Stanford Linear Accelerator Center, Stanford University, Stanford, California, Report No. SLAC-TN-67-6 (1967).

14. R. P. Borghi, A. L. Eldredge, R. H. Helm, A.V. Lisin, G. A. Loew, and R. B. Neal, "Design, fabrication, installation, and performance of the accelerator structure," The Stanford Two-Mile Linear Accelerator, Edited by R. B. Neal (W. A. Benjamin, Inc., New York, 1968), Chapter 6.

15. G. Masek and B. Brown, SLAC Proposal No. 43, Stanford Linear Accelerator Center, Stanford University, Stanford, California (August 1968).

TABLE 1

SUMMARY OF BEAM BREAKUP THRESHOLD IMPROVEMENTS AT SLAC

Date	Comment	Beam Breakup Threshold	
		Computed	Observed
May, 1966	Original operation		20 mA
June, 1967	Quadrupole improvement completed	50 mA [a]	40 mA
October, 1968	Sector 1 detuned by 4 MHz	44 mA [b]	46 mA
January, 1969	Sector 2 detuned by 4 MHz	49 mA [b]	54 mA
July, 1969	Sectors 3, 4, 5, detuned by 2 MHz	57 mA [b]	60 mA
August, 1969	Sectors 10, 13, 16 detuned by 2 MHz	64 mA [b]	65 mA
Future	Sectors 19, 22, 25, 28 detuned by 2 MHz	72 mA [b]	
Future	Sectors 12, 15, 18, 21, 24, 27, 30 detuned by 4 MHz	80 mA [b]	
Future	Additional focusing added in Sectors 24 to 30	86 mA [b]	

(a) Normalized to May, 1966 conditions
(b) Normalized to June, 1967 conditions; recomputed using present best data on rf properties.

TABLE 2

CHOPPED BEAM CAPABILITY

Chopper Frequency	Burst Spacing	Max. Average Pulse Current
40 MHz	12.5 nsec (single bunch)	~10 mA
40 + 20 MHz	25 nsec (single bunch)	~ 8 mA
40 + 20 MHz	25 nsec (several bunches)	~12 mA
40 + 10 MHz	50 nsec (single bunch)	~ 4 mA
40 + 6.6 MHz	75 nsec (single bunch)	~ 3 mA
6.6-20 MHz (continuously variable)	75-25 nsec (several bunches)	1-15 mA (gun limited)
40 + 10 MHz + 50 nsec Gun Pulse	One bunch (~10 psec long)	$\sim 10^9$ electrons

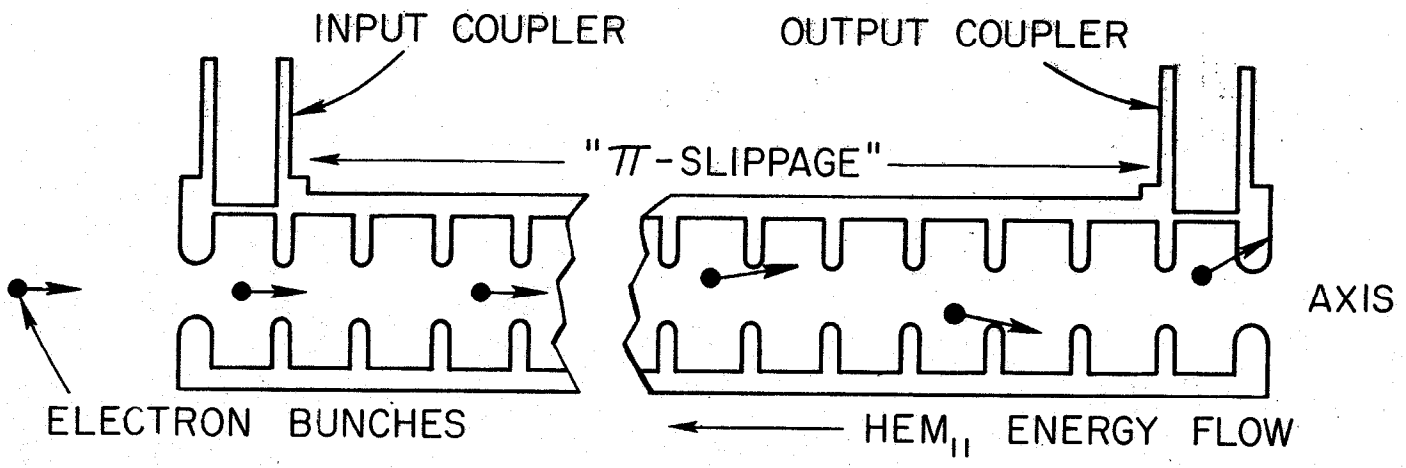

(a)

FIG. 1a--Single accelerator section showing regenerative instability.

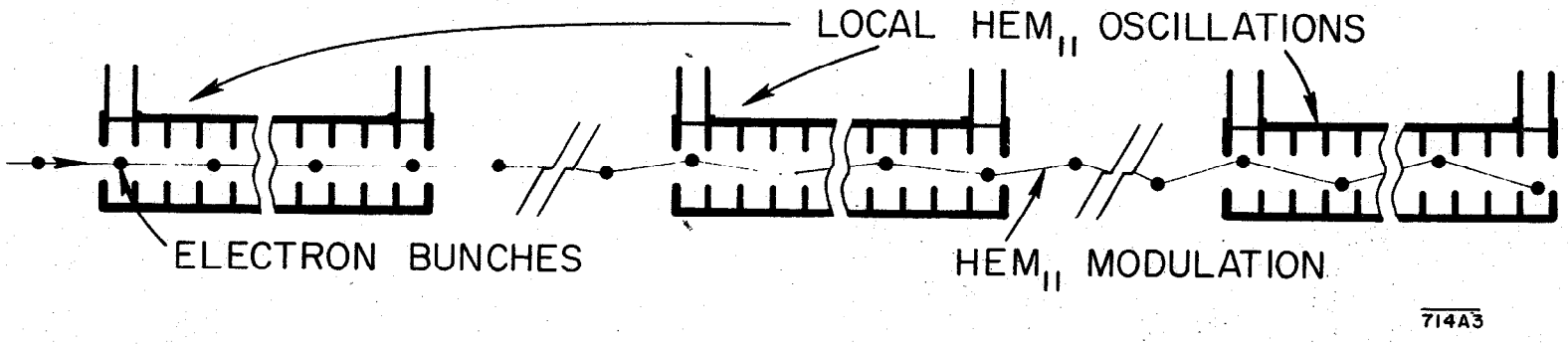

(b)

FIG. 1b--Multi-section accelerator showing cumulative instability build-up.

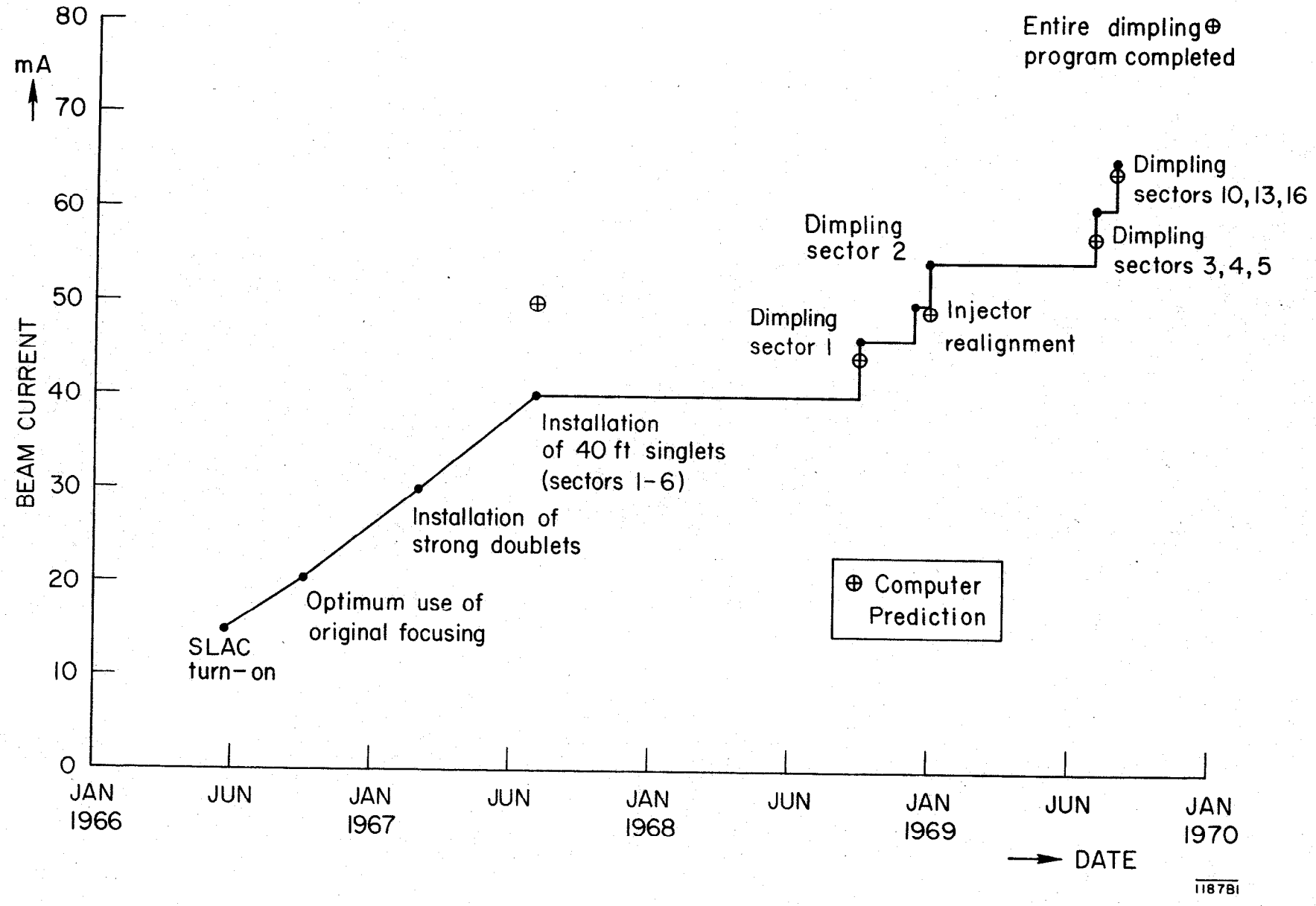

FIG. 2--Improvement of beam breakup threshold at SLAC as a function of calendar time (at 17 GeV and 1.6 μsec pulse length).

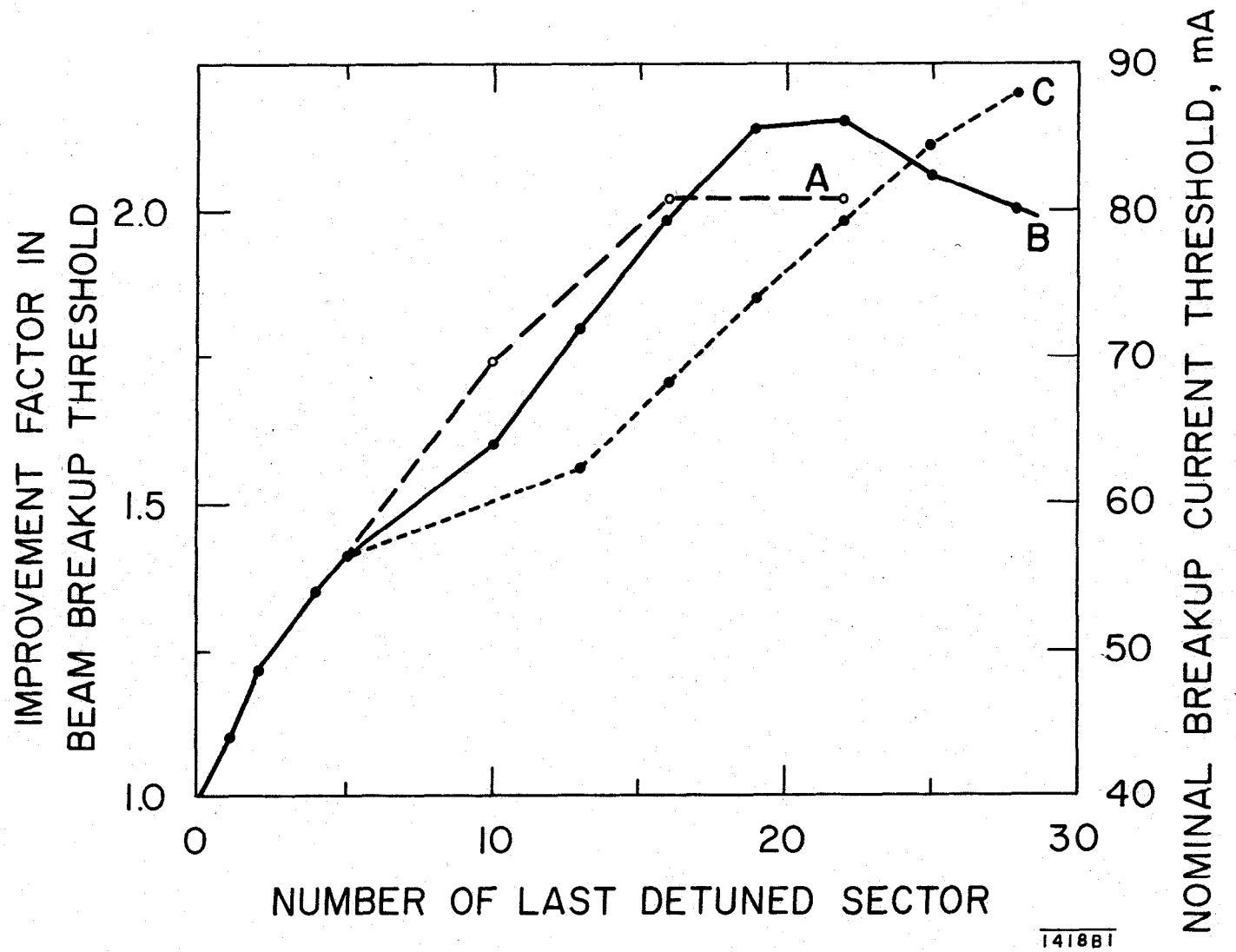

FIG. 3--Computed beam breakup improvement factors for two-mile accelerator with several possible detuning schedules. Schedule C has been adopted.

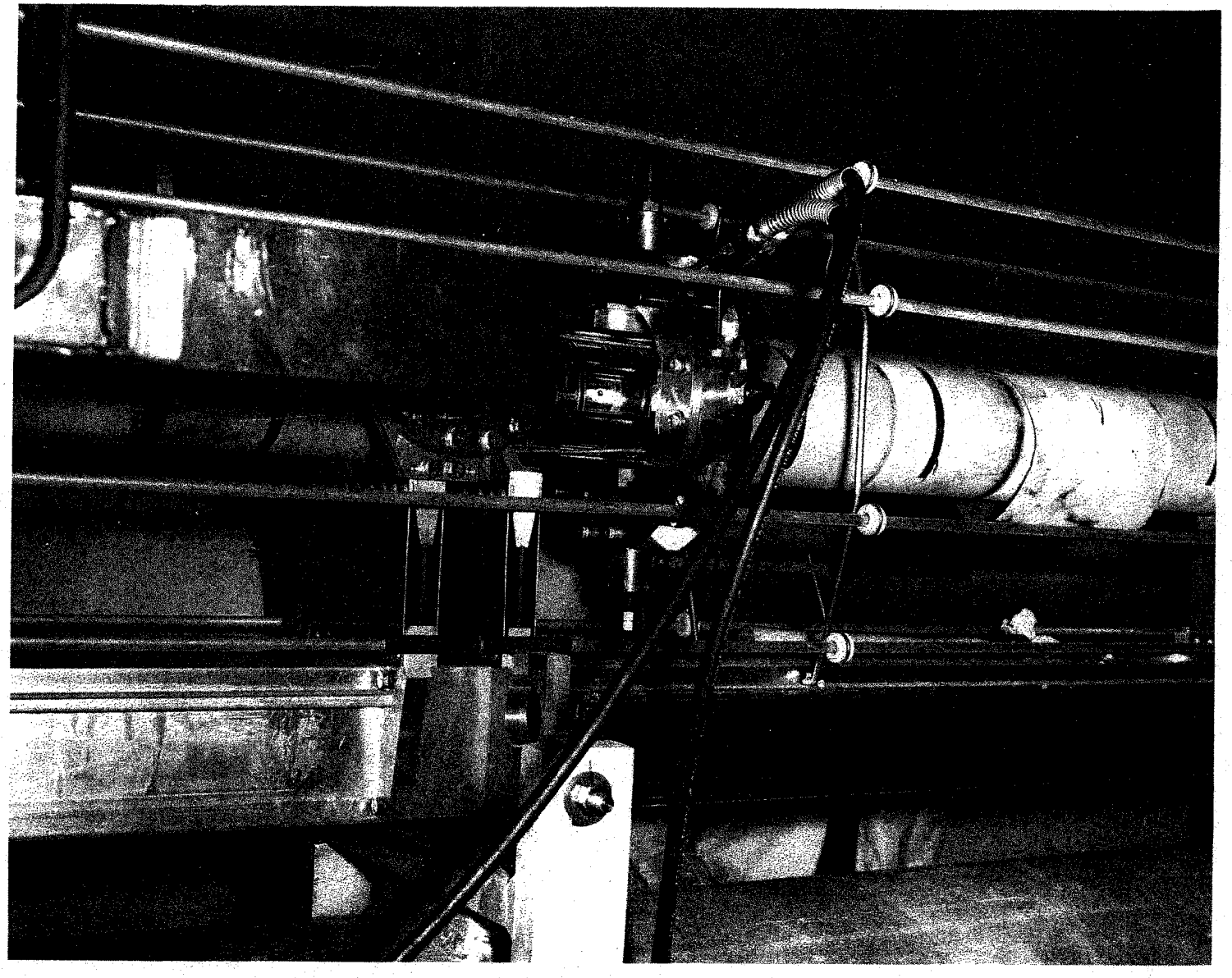

1418A13

FIG. 4--Tool used to detune SLAC beam breakup resonance.

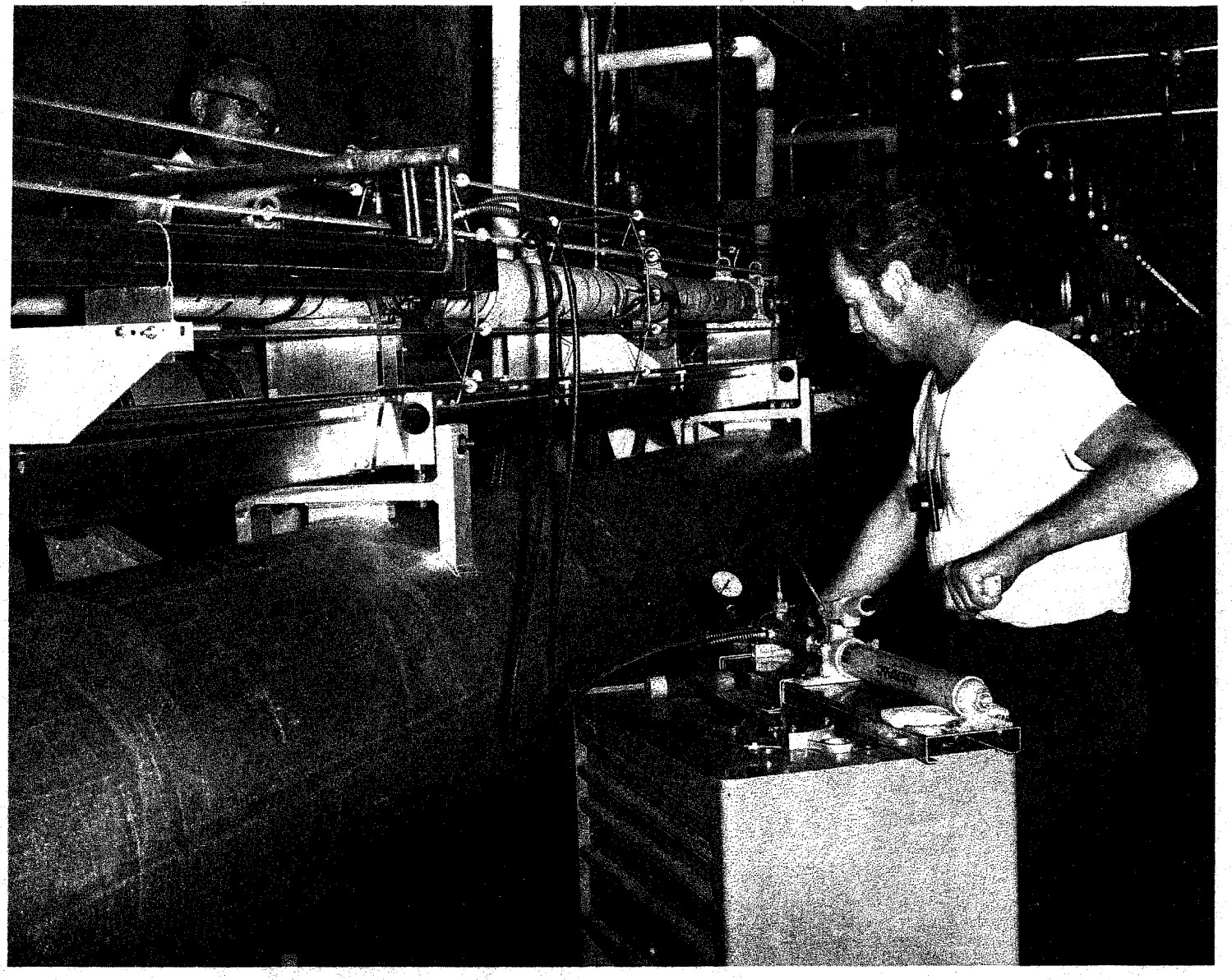

1418A12

FIG. 5--Actual operation of detuning beam breakup resonance.

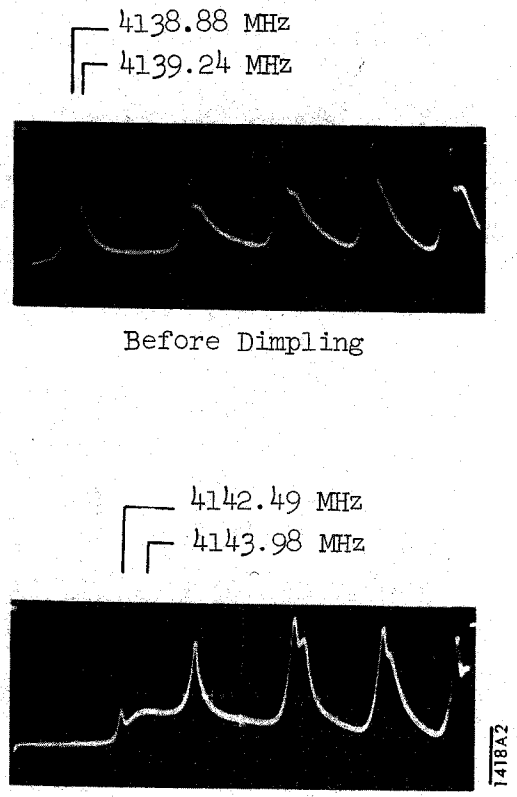

FIG. 6--HEM_{11} resonances in ten-foot accelerator section in Sector 1 before and after detuning.

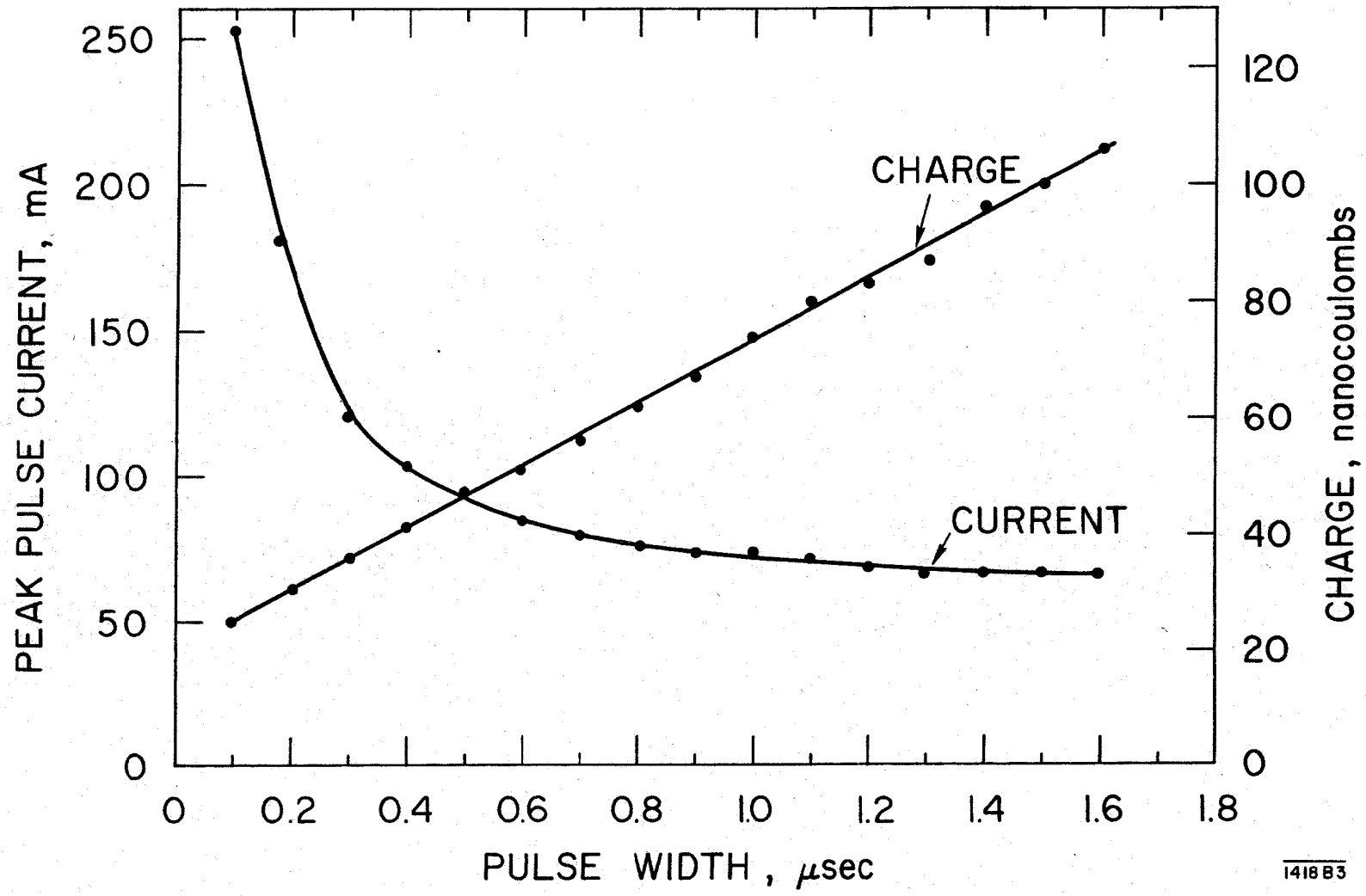

FIG. 7--Experimental beam breakup charge and current vs. pulse length (at 17 GeV and optimum available focusing conditions, August 1969)

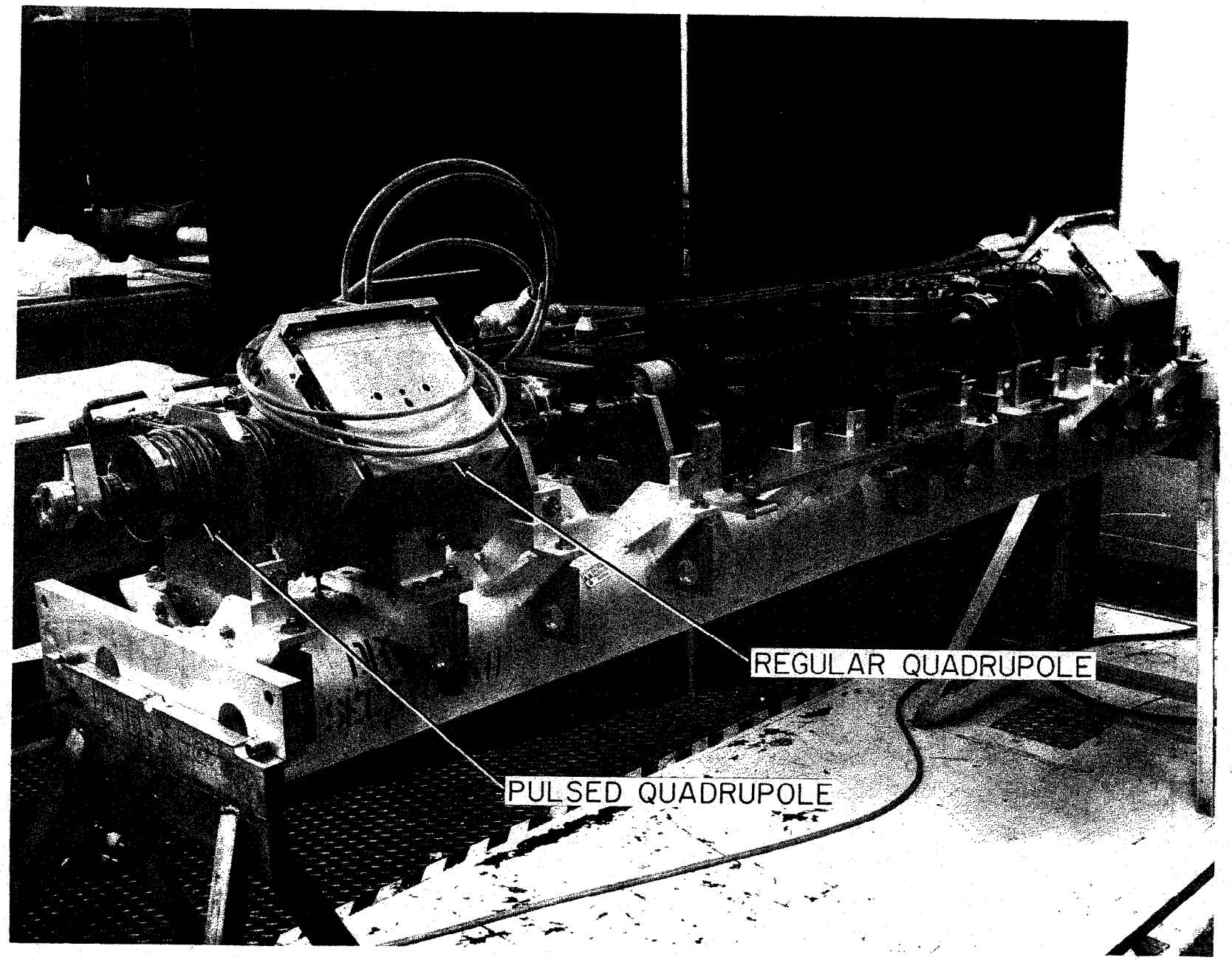

FIG. 8--New drift section in Sector 28 containing both a regular dc quadrupole doublet and a pulsed doublet. 1418A16

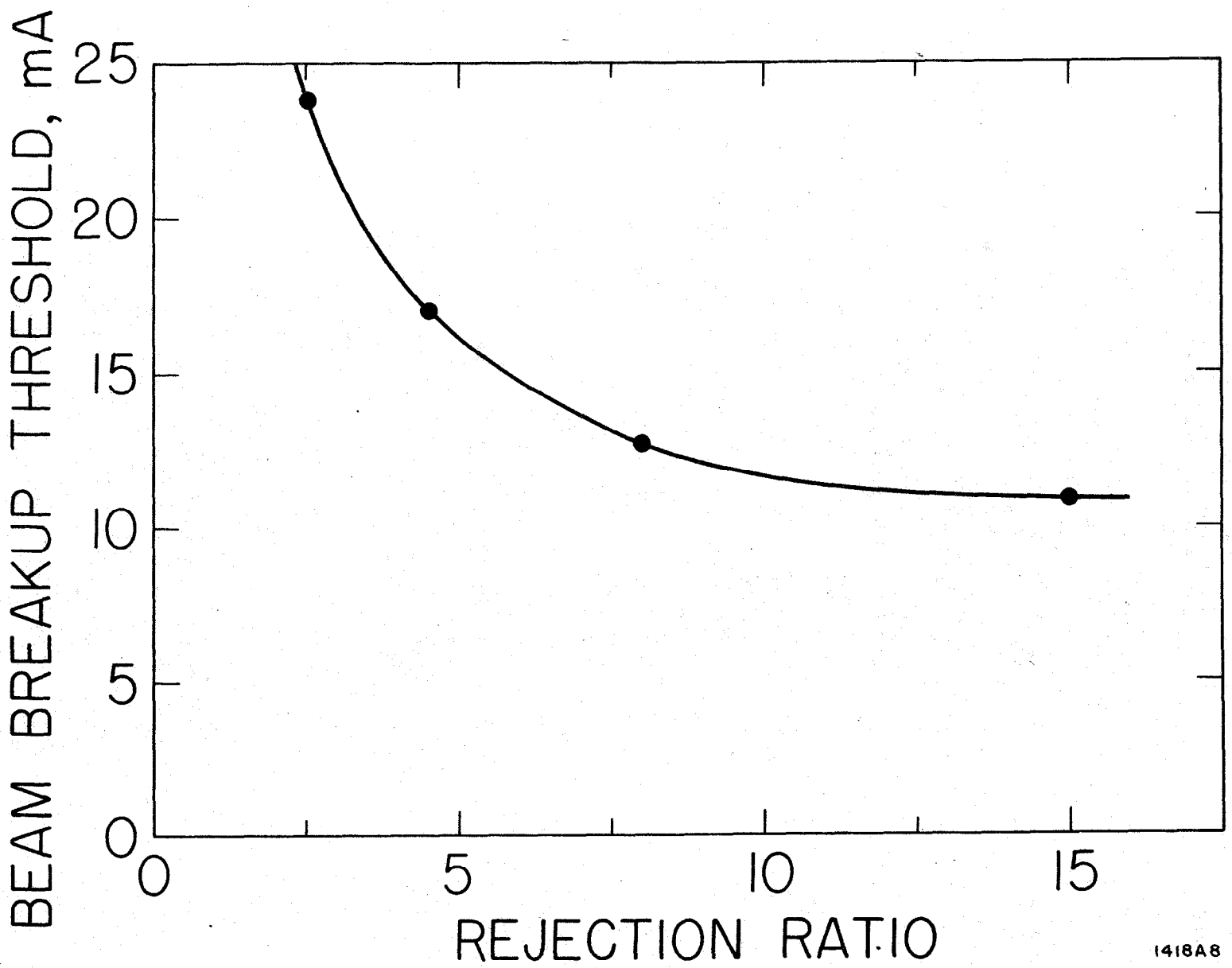

FIG. 9--Beam breakup threshold at end of accelerator as a function of 40 MHz chopper rejection ratio (at 17 GeV and 1.6 μsec pulse length).

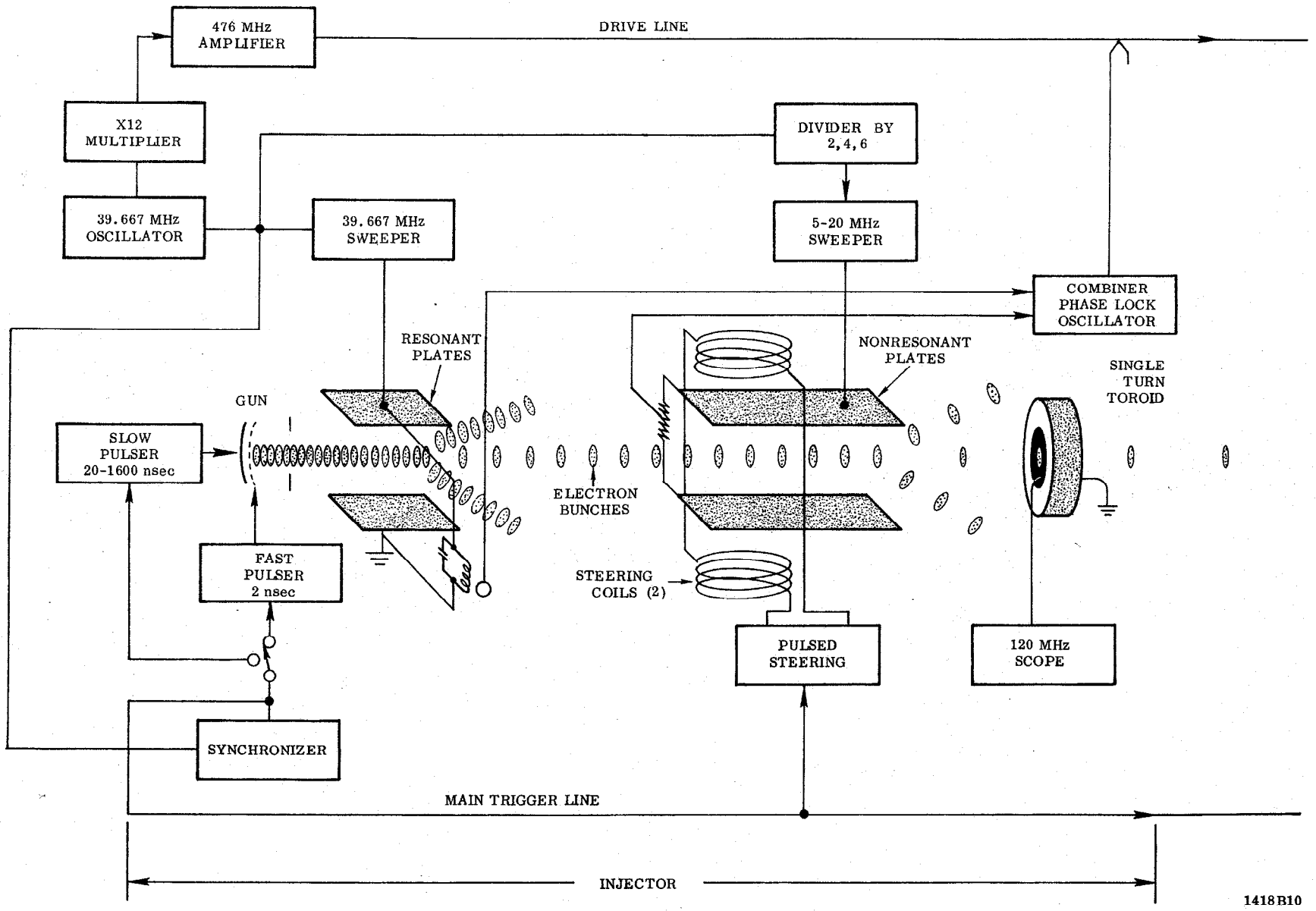

FIG. 10--Block diagram of chopped beam system.

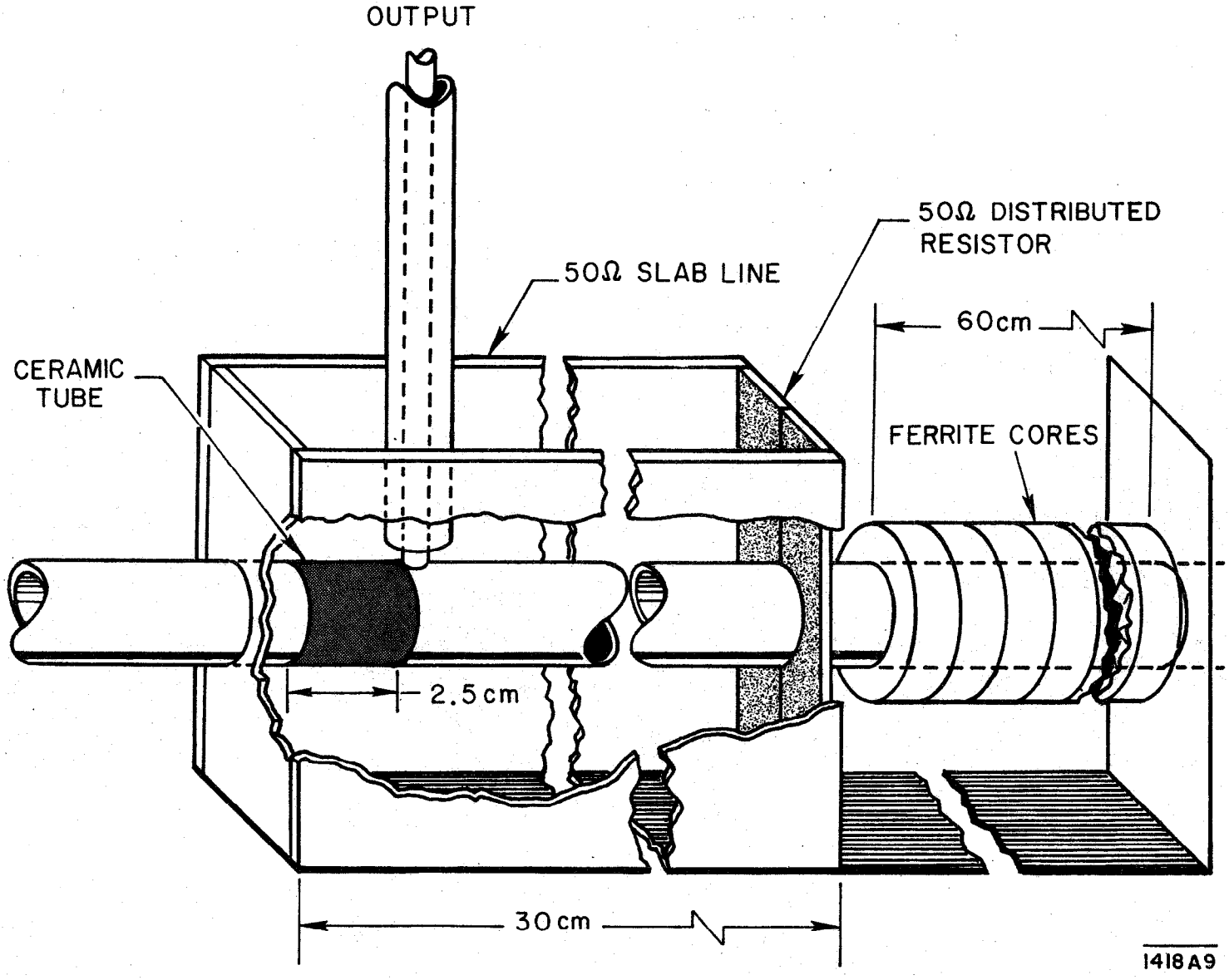

FIG. 11--Fast chopped beam monitor.

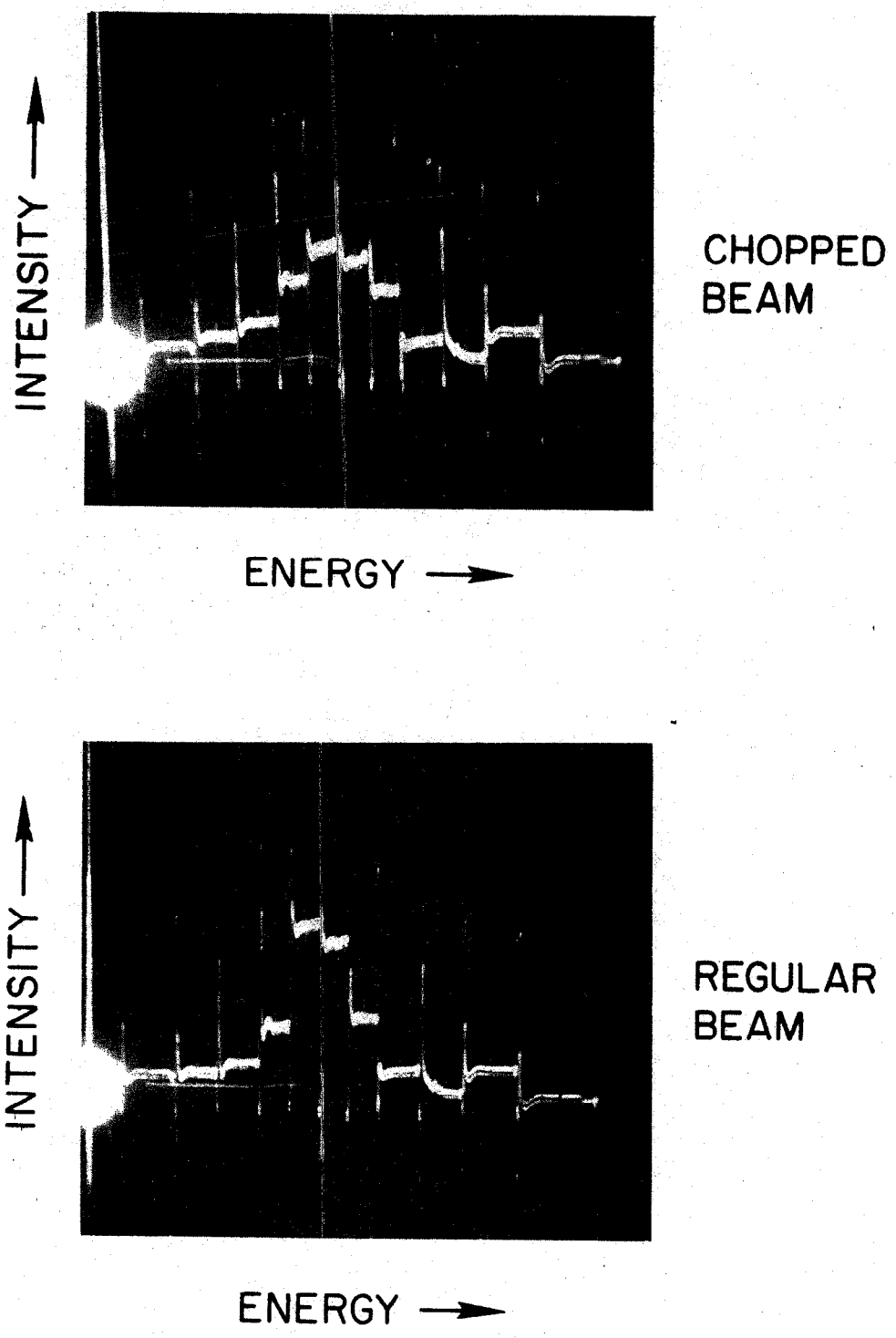

FIG. 12--Comparison of energy spectra for regular and chopped beams of equal intensity (1.4 mA, 10 GeV, 1.6 μsec pulse length). The chopped beam consisted of a train of single bunches spaced 50 nsec apart. The four central foils have a spectrum width of 0.1%, the two subsequent ones on each side, 0.2%, then 0.4%, etc.

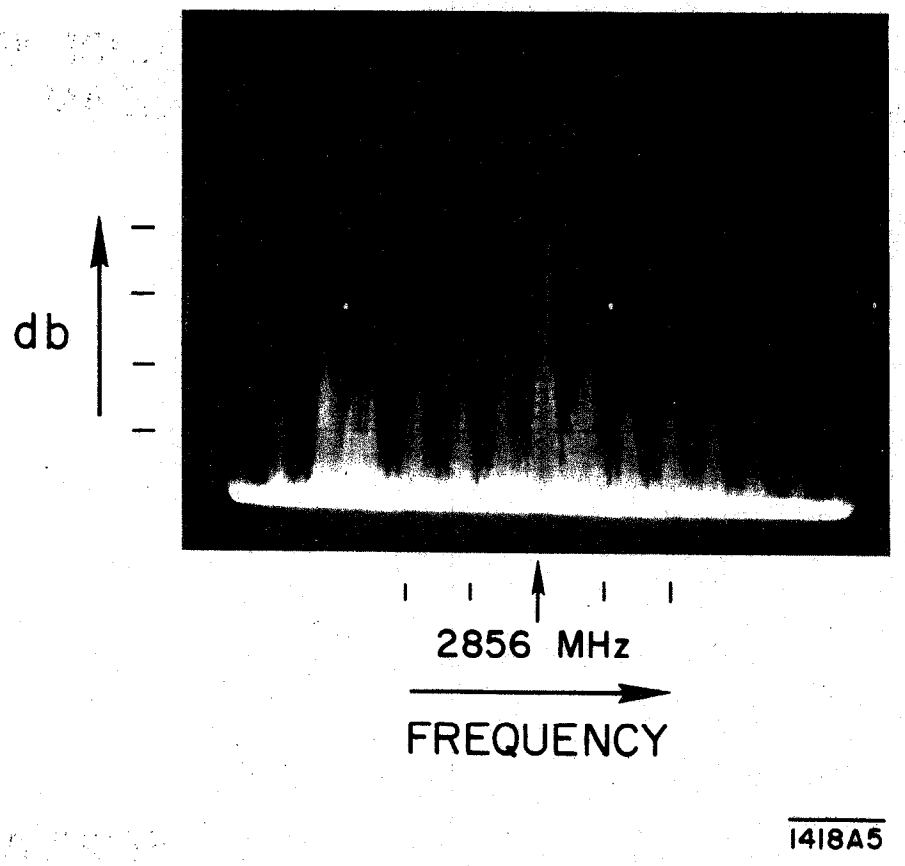

FIG. 13--Spectrum of signal induced in accelerator section by chopped beam with 50 nsec bunch spacing (vertical scale: 10 dB/div; horizontal scale: 30 MHz/div).

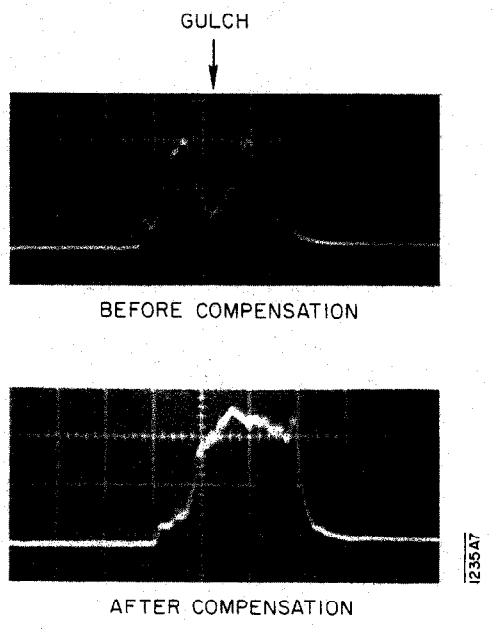

FIG. 14--Gulch-filling on a 17 GeV beam analyzed through 0.2% slits using two klystrons.

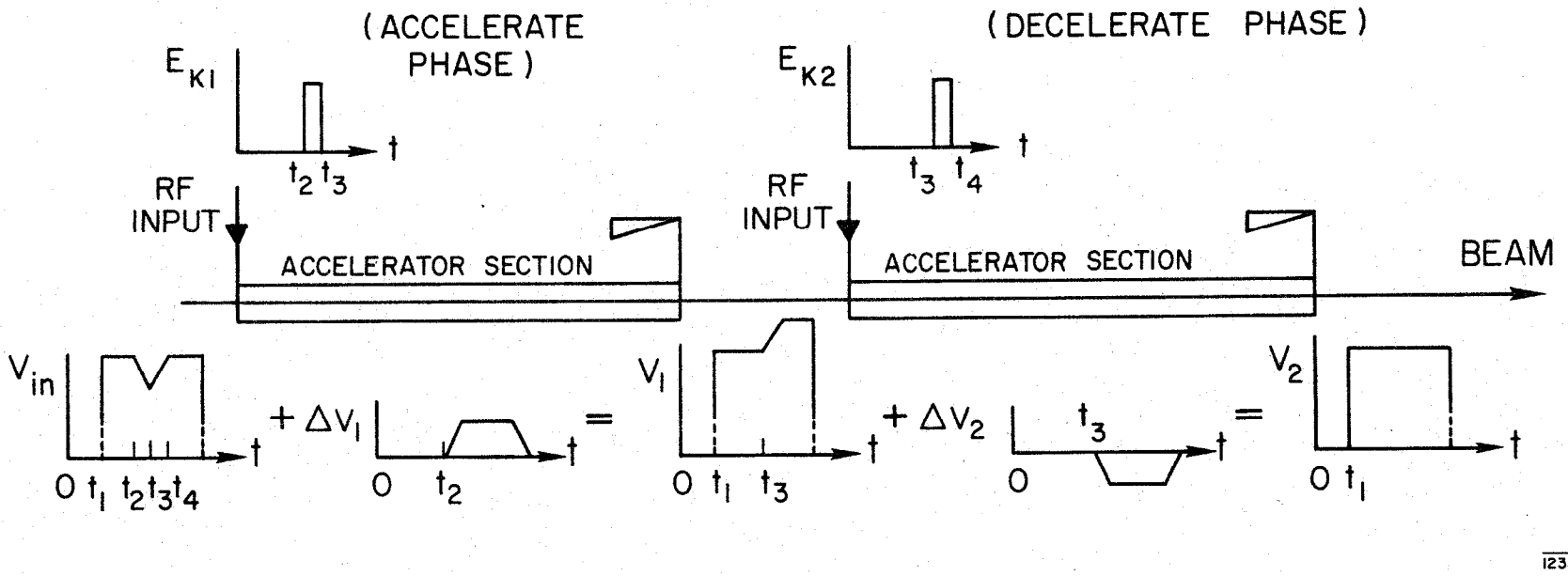

FIG. 15--Illustration of how energy gulch is filled by means of short rf pulses in successive accelerator sections.

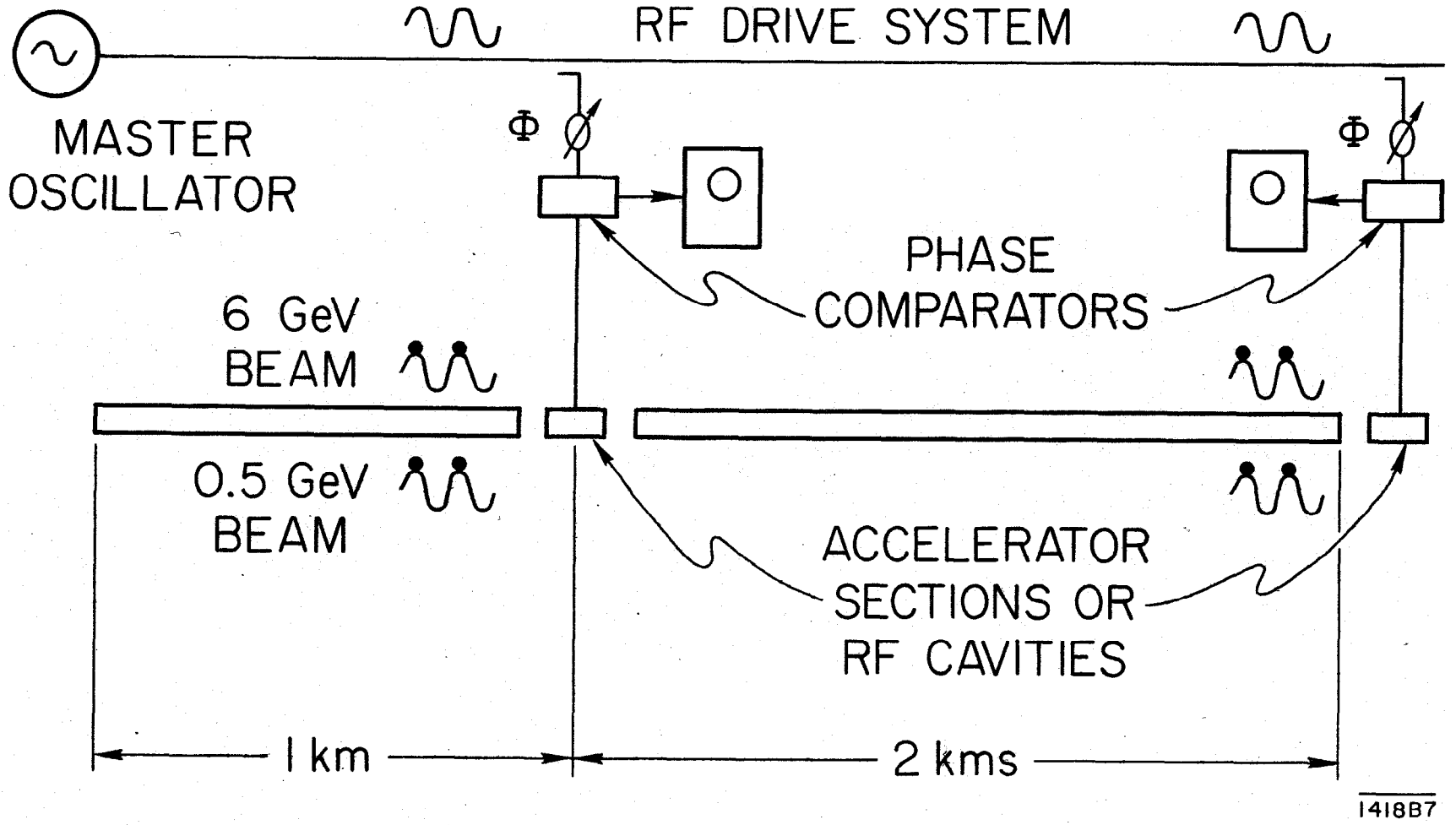

FIG. 16--Illustration of experiment to measure the velocity difference between two relativistic beams of different energies.